Anti-Nociceptive Effect of Sufentanil Polymeric Dissolving Microneedle on Male Mice by Hot Plate Technique

Zeinab Pourmansouri[1], Atefeh Malekkhatabi[2], Maryam Toolabi[3],
Mahsa Akbari[3], Mohammad Ali Shahbazi[3,4*], Ali Rostami[1*]

[1]Department of Pharmacology, School of Medicine, Zanjan University of Medical Sciences, Zanjan, Iran; [2]Department of Pharmaceutical Biomaterials, Tehran University of Medical Sciences, Tehran, Iran; [3]Department of Biomedical Engineering, University Medical Center Groningen, University of Groningen, Antonius Deusinglaan 1, 9713 AV Groningen, the Netherlands; [4]W.J. Kolff Institute for Biomedical Engineering and Materials Science, University of Groningen, Antonius Deusinglaan 1, 9713 AV Groningen, the Netherlands

OPEN ACCESS

ABSTRACT

Background: Despite the widespread use of opioids to manage severe pain, its systemic administration results in side effects. Among the subcutaneous and transdermal drug delivery systems developed to deal with adverse effects, microneedles have drawn attention due to their rapid action, high drug bioavailability, and improved permeability. SUF is an effective injectable opioid for treating severe pain. In this study, we investigated the analgesic effects of SUF using dissolvable microneedles.

Methods: SUF polymeric dissolvable microneedles were constructed through the mold casting method and characterized by SEM and FTIR analysis. Its mechanical strength was also investigated using a texture analyzer. Fluorescence microscopy was applied in vitro to measure the penetration depth of microneedle arrays. Irritation and microchannel closure time, drug release profile, and hemocompatibility test were conducted for the validation of microneedle efficiency. Hot plate test was also used to investigate the analgesic effect of microneedle in an animal model.

Results: Local administration of SUF via dissolving microneedles had an effective analgesic impact. One hour after administration, there was no significant difference between the subcutaneous and the microneedle groups, and the mechanical properties were within acceptable limits.

Conclusion: Microneedling is an effective strategy in immediate pain relief compared to the traditional methods. ***DOI: 10.61186/ibj.4062***

Corresponding Authors:

Mohammad Ali Shahbazi
W.J. Kolff Institute for Biomedical Engineering and Materials Science, University of Groningen, Antonius Deusinglaan 1, 9713 AV Groningen, the Netherlands; Tel.: (+31- 050) 363 9111; Fax: (+31-050) 363 9111; E-mail: m.a.shahbazi@umcg.nl

Ali Rostami
Department of Pharmacology, School of Medicine, Zanjan University of Medical Sciences, Zanjan, Iran; Tel.: (+98-024) 33140272; Fax: (+98-024) 33140272; E-mail: rostami@zums.ac.ir

List of Abbreviations:
DMN: dissolving microneedle; **FITC:** fluorescein-5-isothiocyanate; **PBS:** phosphate-buffered saline; **FTIR:** fourier transform infrared spectroscopy; **H&E:** hematoxylin-eosin; **K/X:** ketamine/xylazine 20%/80%; **MPA:** maximum possible analgesia; **N/S:** normal saline; **PF:** parafilm M®; **PVP:** polyvinylpyrrolidone; **RBC:** red blood cells; **SC:** subcutaneous; **SEM:** scanning electron microscopy; **SUF:** sufentanil; **UV-Vis:** ultraviolet-visible

INTRODUCTION

Pain is a sensory and emotional experience associated with actual or potential tissue damage[1] and considered one of the most common complaints of patients. Opioids are among the drugs widely used to treat pain. Based on the analgesic effect of opioids, they can be classified as strong (SUF and fentanyl), moderate (partial agonists and mixed agonist-antagonists), and weak (codeine)[2]. Transdermal administration of potent opioids may provide long-term effective analgesia for patients with cutaneous nociceptive and neuropathic pains[3].

SUF is a fentanyl analog proven to be ~7-10 times more efficient than fentanyl and ~1000 times more effective than morphine in animal studies[4]. It possesses advantages including high potency, high therapeutic index[5], and shortened duration of action[6]. Its high affinity toward opioid receptors[7] corresponds to its analgesic effect, even at low concentrations[8]. Lipophilic nature of SUF results in its rapid distribution in tissues[9], with a distribution time of ~1.4 min and redistribution time of 18 min[10]. The metabolization process of SUF involves dealkylation and demethylation in the liver via cytochrome P-450 3A4[11] and the small intestine[4], which converts it into inactive metabolites[9] excreting in the urine[12]. Due to its poor oral bioavailability, reconsidering its oral administration in small amounts is advisable unless the sublingual formulation demonstrates good absorption and acceptable efficacy in controlling pain when the patient is awake and conscious[13]. However, when supplements depend on caregiver prescribing, there is a risk of long-term "analgesic gaps"[14]. Among different administration routes, subcutaneous injection is considered to be safe and practical, providing effective analgesia with minimal side effects[15]. As a method of subcutaneous administration of SUF, the implanted osmotic pump has demonstrated a 100% bioavailability. Nevertheless, in this administration route, the drug absorption is slower than that of the subcutaneous method, which requires specialist intervention, as do its intravenous forms[16]. Other transdermal delivery systems, such as TRANSDUR™ and the Labtec GmbH transdermal system, are currently undergoing clinical trials and are highly suitable for transdermal delivery of SUF because of the low molecular weight, high potency, and high lipophilicity of this drug[17]. Since not all drugs possess the necessary physicochemical properties to penetrate the stratum corneum barrier effectively, transdermal drug delivery presents a challenge. If this barrier is broken, percutaneous delivery may be considered an excellent method of drug delivery due to its low cost[18], relative safety[16], acceptable therapeutic efficacy by circumventing first-pass metabolism, lack of pill fatigue[19], and reducing the risk of injection site infections[18]. One way to achieve these goals is to use microneedles[16].

Microneedles are micrometer-sized needles that line the surface of small patches, offering advantages over subcutaneous or other transdermal drug delivery mechanisms[20]. Microneedles with a diameter of 1000 μm easily penetrate the SC and effectively deliver drugs[21]. Dissolving needles are the best choice for microneedles because they are easily designed and biodegradable polymers, making them suitable for sustained drug delivery[14,22], drug loading[22] and one-step administration[23]. They also leave no biologically hazardous residues after administration[24], and they regulate drug release by controlling the dissolution rate of the microneedle polymer[22].

In the current study, we fabricated a SUF DMN patch for cutaneous nociceptive pain control, using the hot plate technique in mice and evaluated the efficiency of the DMN compared to subcutaneous administration.

MATERIALS AND METHODS

Materials

PVP K90, FITC, and PBS tablets were purchased from Sigma-Aldrich (Missouri, USA) and SUF citrate from Tofigh Daru (Tehran, Iran). Glycerol (glycerin) and trypan blue were provided by Merck company (Darmstadt, Germany). Ethanol was purchased from Kimia Alcohol Zanjan (Iran), methanol from Daejung company (South Korea), and polydimethylsiloxane microneedle molds and MPatchTM Mini Applicator (5-15 mm in diameter) from Microprint Technologies Pte Ltd. (Singapore).

Fabrication of SUF DMNs

Microneedles were fabricated by the mold casting method using PVP as the casting material. A 18% (w/v) solution of PVP in deionized water was mixed with 300 μg/ml of SUF dissolved in 100 μl of methanol and 0.3% glycerol (w/w). Next, 1,000 μl of this solution was added to polydimethylsiloxane micromold and centrifuged at 4,500 ×g for 30 min to depressurize the solution in the mold cavities (the shorter centrifugation time or speed, the more air bubbles at the end of the preparation). This procedure was performed twice. Afterwards, a one-hour resting period was implemented to allow the liquid to penetrate the cavities. Another layer of polymer containing the drug was placed in the mold and rested for 1 h. Thereafter, two layers of polymer without the drug were added to the mold as the backing layer of microneedles to fill the space. The micromold was then placed in a desiccator for 36 h to

accelerate drying. Finally, the microneedles were detached from the molds (the cooler the weather, the later the drying and the fewer the bubbles). To observe the complete morphology of the needles, we employed optical microscopy with a 10× and 40× objectives; (Olympus, Japan) and SEM (MIRA3TESCAN-XMU, LVSTD detector, Germany). Microneedles characteristics = 10 × 10 arrays, height = 8 μm, base = 200 μm, pitch to pitch = 500 μm; pyramid shape). The fabricated microneedles were stored in a desiccator until further use to protect them from the humidity of the environment. In all stages, to ensure that the drug does not affect the performance of the microneedles, the drug-free microneedle (PVP DMN) was compared with the microneedle containing the drug (SUF DMN).

Morphological analysis by SEM

The microneedles were fixed to aluminum rods with adhesive carbon tapes and then examined under SEM to determine their morphology and topography. Microphotographs of the patches were evaluated to determine the morphology and dimensions of the microneedles.

FTIR analysis

To confirm, identify and evaluate the functional group interactions between the drug and excipients, pure PVP, pure SUF, and combination of PVP and SUF were analyzed by FTIR. The infrared spectra of the samples were recorded using a FTIR device (PerkinElmer Frontier, USA) with a Diamond ATR holder in a wavenumber range of 500-4000 cm^{-1}.

Compression test assay

The mechanical strength was investigated using a texture analyzer (Santam Co., Iran; model DBBP-20, capacity = 29 kgf, and RGO = 3mv/v). The patch was attached to the flat probe with double-sided adhesive tape. The axial force was applied by moving the probe against a rigid stainless steel base plate in the vertical direction with a force of 0 N to 73 N and a speed of 1 mm/min and kept for 90 s. Following photographing the DMNs before and after the procedure, the height of the microneedles was measured using Image J software through the below formula in which the original height of the needles is [H1] and the height of the needles after compression is [H2].

$$\text{Height reduction } (\%) = [\frac{H1-H2}{H1}] \times 100$$

In vitro and in vivo insertion assay

PF (a mixture of hydrocarbon wax and polyolefin) was used as a skin model to observe the penetration ability of the patches. PF was folded into eight layers without being stretched. Then the patch was pressed in PF using an applicator with thickness of 127 μm for each layer and the size of 3 × 3 cm. The PF was then unfolded, and the number of pierced holes in each layer was counted using an optical microscope (×40, Olympus BX61, Japan) to determine the percentage of penetration using the following formula:

$$\text{Penetration } (\%) = (\frac{Number\ of\ penetrated\ needles}{all\ needles\ penetrated}) \times 100$$

To do the in vivo penetration test, a trypan blue-loaded patch of PVP and SUF DMN was inserted into the dorsum of the anesthetized mouse as a model for human skin. The patches were removed from the skin and then the skin area where the patches were inserted was biopsied and placed in 10% formalin for fixation. The sample underwent an H&E test to determine if the microneedles could effectively penetrate the SC of the skin. The experiment was carried out in triplicates.

Study of skin irritation and microchannel closure time

Male BALB/c mice (Mus musculus, 6-8 weeks old) were gifted from Pharmacology Department at Medical School of Zanjan University of Medical Sciences. To acclimatize, animals were housed in a temperature-controlled room (25 ± 2 °C) for 7 days. During this laboratory condition with a 12 h light-dark cycle, animals were allowed to access food and water freely. After mice were anesthetized with ketamine/xylazine (20:80%), their skin was fixed, and a microneedle was placed on the skin using a small flat metal piece as a supporter. At intervals of 15 min, 1, 8, and 24 h after the removal of the microneedle from the skin surface, the animals were euthanized using a K/X overdose, and the skin of the area was removed and fixed in formalin. H&E staining was performed to investigate the side effects and skin regeneration post microneedles treatment. The experiment was carried out in triplicates.

Confocal microscopy analysis

Fluorescence microscopy was used in vitro on rat skin to measure the penetration depth of microneedle arrays. The FITC diffusion was also used throughout the skin layers to show the capability of microneedles in delivering the drug into the dermis and blood vessels. The FITC/PVP microneedles were inserted into the rat skin using an applicator and then held in place for 1 h before being fixed in the skin with a TG band-aid for 4 and 8 h. Subsequently, the fluorescence signal in the skin was imaged using a confocal microscope (Nikon Eclipse TiE, 2011, Nikon, Osaka, Japan) to determine the depth of insertion and the distribution of

fluorescence in the skin. Finally, confocal microscopic images of fluorescent DMN were obtained throughout the entire thickness of rat skin at 1, 4, and 8 h; the images of each layer of the skin, up to a depth of 2400 µm, were obtained at 50-µm intervals.

In vitro release assay

To evaluate the release profile of the microneedles, 10 dried microneedles containing the drug were immersed in 5 ml of PBS (pH 7.4), to simulate the pH of skin interstitial fluid and then placed on a magnetic stirrer (40 rpm). The sample was kept at 37 °C. At predetermined time points (30 s, 1, 2, 5, 10, 20, 30, 45, 60, 90, and 120 min, 3, 4, 5, and 6 h), 500 µl of the solution was withdrawn, and 500 µl of fresh PBS without drug was simultaneously added to the environment to equilibrate and maintain the sink condition. Then the absorbance of the samples was read at 228 nm using a UV/Vis spectrometer (T80+, PG Instruments, China) and placed into the SUF calibration curve to obtain the cumulative release graph and determine the amount of the drug.

Hemocompatibility test

To determine the hemocompatibility properties of PVP and PVP/SUF polymers, lyophilized samples were tested at different time points with consecutively increasing concentration of the compounds (50, 100, 200, and 400 µg/ml) with water as a positive control (100% hemolysis) and PBS (pH 7.4) as a negative control (0% hemolysis). Fresh whole blood sample from a healthy volunteer was collected in an anticoagulated tube and used within 2 h of collection. Next, 20 ml of PBS (pH 7.4) was lightly added to 10 ml of whole blood sample and centrifuged at 3000 ×g for 6 min. The supernatant was discarded, and the precipitated RBC was collected and washed five times with a 1:2 ratio of RBCs to PBS. The PBS was then added to the RBCs to reach a concentration of 5% v/v and incubated with samples of PVP and PVP/SUF polymers at 37 °C. After incubation for 1, 4, 8, and 24 h, the tested samples were centrifuged at 4000 ×g for 5 min, and 150 µl of the supernatant was transferred to a 96-well plate. The optical density of the samples was measured at 540 nm using an ELISA reader (Tecan Infinite M200 microplate reader, Austria). The percentage of non-hemolyzed erythrocytes was determined using the following equation. The experiment was performed in four replicates.

$$\text{Non-hemolysis (\%)} = \left(1 - \left[\frac{(Absorbance\ of\ sample - Absorbance\ of\ negative\ control)}{(Absorbance\ of\ positive\ control - Absorbance\ of\ negative\ control)}\right]\right) \times 100$$

In vivo toxicity assay

Two weeks after treatment, mice groups, including PVP DMNs, SUF DMNs, SUF and N/S (control group), were anesthetized using ketamine/xylazine, and whole blood sample (1.5 ml) was collected via cardiac puncture. The serum level of blood urea nitrogen, creatinine, lactate dehydrogenase, alkaline phosphatase, total protein, albumin, aspartate and alanine transaminase, calcium, phosphorus, and the number of blood cells were measured. Moreover, major organs (liver, kidneys, and spleen) of animals from four experimental groups were harvested and stained with H&E to evaluate histopathological changes.

In vivo transdermal dissolution

A dissolution experiment was performed on live rats and mice. Animals were anesthetized via K/X injection and shaved. Afterward, the patches were applied to the animal's skin using an applicator, with and without a supporter, small flat metal piece, for both microneedle groups. Thumb pressure was used for fixing the applicator in the injection era. Following the insertion, the microneedles were rapidly dissolved in the skin's interstitial fluid. At various time points (0, 2, 5, 10, 20, 30, and 45 min), the patches were removed and visualized under a bright-field microscope for measuring the length of inserted arrays. Moreover, SEM images were obtained to achieve a precise view of the dissolution.

Hot plate test

The analgesia hot plate test was performed as described previously[25]. The experimental study was conducted on adult male mice weighing 18 and 22 g. All animals were kept under standard conditions and acclimated to the environment before the experiment to prevent the stress caused by environmental changes. The mice were divided into four groups of six mice each. Then N/S, SUF (0.3 µg), SUF DMN (0.3 µg of SUF), and PVP DMN were administered subcutaneously to the control, SUF SC, SUF DMN, and PVP DMN groups, respectively. Mice were placed on a hot plate (Stoelting, USA) at 0, 5, 15, 45, 60, 240 and 360 min. The jump time of the mice on the surface of the hot plate (55 °C ± 0.1) was recorded. The cut-off time was 20 s. The percentage of MPA was calculated for each group using the equation as follows:

$$\text{MPA (\%)} = \left(\frac{(Reaction\ time\ for\ treatment - reaction\ time\ for\ control)}{(Cut-off\ time\ (20) - reaction\ time\ for\ control)}\right) \times 100$$

Statistical analysis

Data were analyzed using SPSS version 26. Data are presented as mean ± standard deviation. In all cases, a one-way ANOVA was performed with Tukey's post hoc test, and $p < 0.05$ showed a significant difference among the experimental groups.

RESULTS

Fabrication and characterization of SUF DMNs

SUF DMN was fabricated by a typical micromolding process (Fig. S1A). SEM analysis revealed a pyramidal shaped structure. Each patch consisted of 100 needles (10 × 10 array), with a length of ~800 μm (Fig. S1B). Based on the standard curve of SUF, the amount of the drug in each patch was nearly 0.3 μg. The FTIR spectrum was examined between 500 and 4000 cm^{-1} to identify the functional groups of the DMN polymers and evaluate interactions between the compounds. Starting from pure PVP, the peak absorption at 1580 cm^{-1} could be referred to the stretching vibration of C=O in the carbonyl group. The peaks for the C-H stretching vibrations were observed at 2932 and 2885 cm^{-1}, and the bending vibration was at 1428 cm^{-1}. In addition, peak at 1284 cm^{-1} was identified as the C-N bending vibration of the pyrrolidone structure. Due to the hydrophilic nature of PVP, the peak at 3432 cm^{-1} was associated with the OH stretching vibration. FTIR of the pure SUF showed the following peaks: 650 and 570 cm^{-1} (stretching of the C-S group), 1418 cm^{-1} (bending of C-H in the C-H$_2$ group), 1375 cm^{-1} (bending of C-H in the C-H$_3$ group), 1177 cm^{-1} (stretching of C-N group), 1109 cm^{-1} (stretching of C-O group), 1610 cm^{-1} (aromatic ring), 1591 cm^{-1} (stretching of C=O group), 2932 and 2824 cm^{-1} (stretching of C-H group), and 3462 cm^{-1} (stretching of OH group). According to the FTIR peaks of PVP/SUF, the combination of the two substances showed a slight shift, and the reaction of the two substances together resulted in the formation of a stretching NCO group at 2133 cm^{-1}. The observation of all the SUF peaks also suggested that the process of fabrication and the ingredients of DMN had no deleterious effects on the structure of the drug (Fig. S1C).

Determination of the mechanical strength of PVP MN arrays

The mechanical strength of the PVP MN arrays was measured using a compression test involving various predetermined forces generated by a tissue analyzer. The height reduction of PVP DMN (without drug) ranged from 6.87% to 50.18% of the original height when forces between 15 and 60 N/patch were applied. The height reduction of SUF DMN was in the range of 9.11%-74.63% when the same forces were used (Fig. 1). The breaking force of both DMNs was 73 N/patch. The DMN patches showed a proper potential to resist forces greater than 9 N/patch (0.09 N/needle) with negligible height reduction.

Penetration of DMNs into PF layers and animal skin

The microneedles were subjected to in vitro skin penetration test using paraffin. SUF DMNs and PVP DMN penetrated the third and fourth layers of PF (Fig. 2A). As the thickness of each layer of PF is ~127 μm, the total puncture depth for each of our DMNs was ~381 and 508 μm, respectively (Fig. 2B), which represents 47.625% and 63.5% of the total height of deployed DMN arrays. This result shows that DMNs can penetrate the SC (~10 up to 20 μm) and easily pass through the skin. To evaluate the in vivo insertion capability of DMNs, we administered trypan blue-loaded DMNs to the full thickness of hairless animal skin. The needles were successfully inserted into the skin and passed SC (Fig. 2C). We also used confocal microscopy to determine the depth of permeation. As shown in Figure 2D, FITC was able to penetrate the deeper layers of the skin over 8 h, reaching depths of ~700, 1,200, and 2,000 μm at 1, 4, and 8 h, respectively. It was also able to reach the depth of the dermis and blood vessels excellently, showing that our DMN can effectively transport its drug content to the target site and successfully penetrate the skin.

Examination of skin irritation and inflammatory reaction

After insertion and removal of microneedles at predefined times, we examined local skin irritation and inflammatory reactions. Neither apparent erythema nor inflammatory reactions were observed at the administration site, although mild and transient skin irritation was detected (Fig. 3A). We also evaluated the transient disruption of SC by the formation of micropores. Based on ex vivo histologic studies of the skin for 24 h (Fig. 3B), the depth of the micropores decreased over the mentioned time, and the resealing process began within 1 h of insertion, and completed after 24 h.

Cumulative release profile of SUF DMN

The cumulative release profile of SUF showed an initial release percentage of nearly 60% within 15 min (Fig. 4). Also, almost 84% of SUF was released into the medium within 25 min of initiation. Finally, after 45 min, the cumulative amount of SUF remained almost unchanged, with a final cumulative release percentage of 100% of SUF.
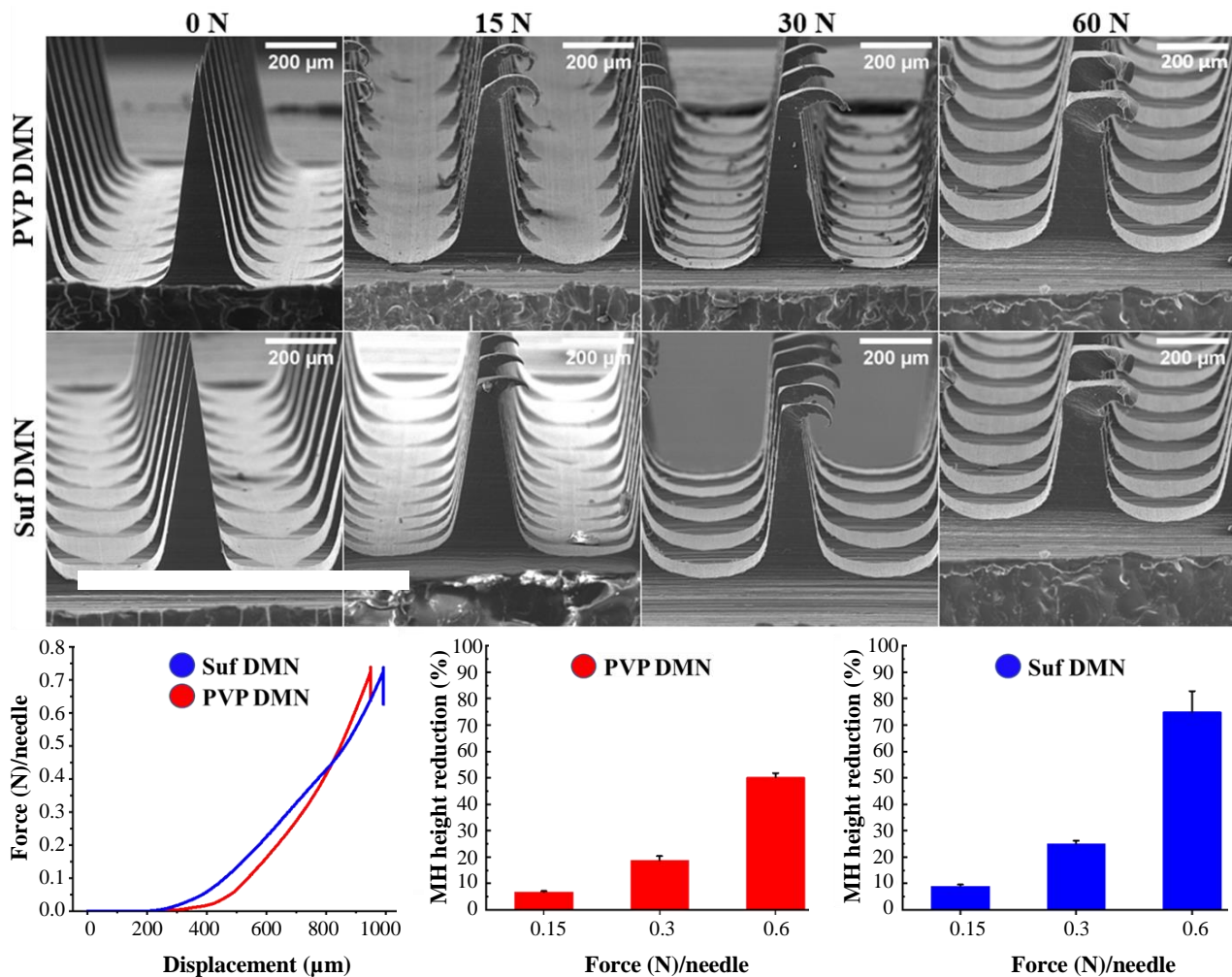
Fig. 1. Mechanical performance of PVP and SUF DMNs, and SEM micrographs of microneedle patches at different forces. The breaking force of the DMNs is 73 N/patch.

Hemocompatible properties of MNs

The hemolysis test exhibited satisfying hemo-compatibility at all concentrations og PVP and PVP/SUF polymers. The results for non-hemolyzed erythrocytes were >99%, in contrast to the positive control, which showed 100% erythrocyte lysis (Fig. 5A). The transparency of the supernatant in all tubes (Fig. 5B) validated our data, as it closely resembled that of the negative control group (zero RBC lysis).

Biocompatible properties of DMNs

Toxicity studies were conducted to assess hematological parameters, serum biochemical indices, as indicators of the systemic effects of DMN. Our study found no statistical difference between the control and treated groups for the above parameters (Fig. 6A; $p >$ 0.05). Histological examination of major organs, including the spleen, liver, and kidney, revealed no noticeable histopathological abnormalities or damage in the experimental groups compared to the control group (Fig. 6B).

Transdermal dissolution of DMNs

The dissolution data showed that when a supporter (small, flat metal piece) was used, almost 50% of the arrays were dissolved in the skin of both animals (rats and mice) within 5 min after insertion. Of note, they were completely dissolved within 20 min. Without a supporter, almost 85% of the arrays were dissolved within 40 min. These observations exhibit that placing a hard object under the skin may assist the microneedle in better skin penetration and faster dissolution (Fig. 7A). Comparing the two different groups of animals (rats and mice) displayed that varying skin thicknesses at the same time point had different degrees of dissolution (Fig. 7B). In other words, there was a significant difference between the mice and rats and also between the animals with and without supporters ($p < 0.05$).
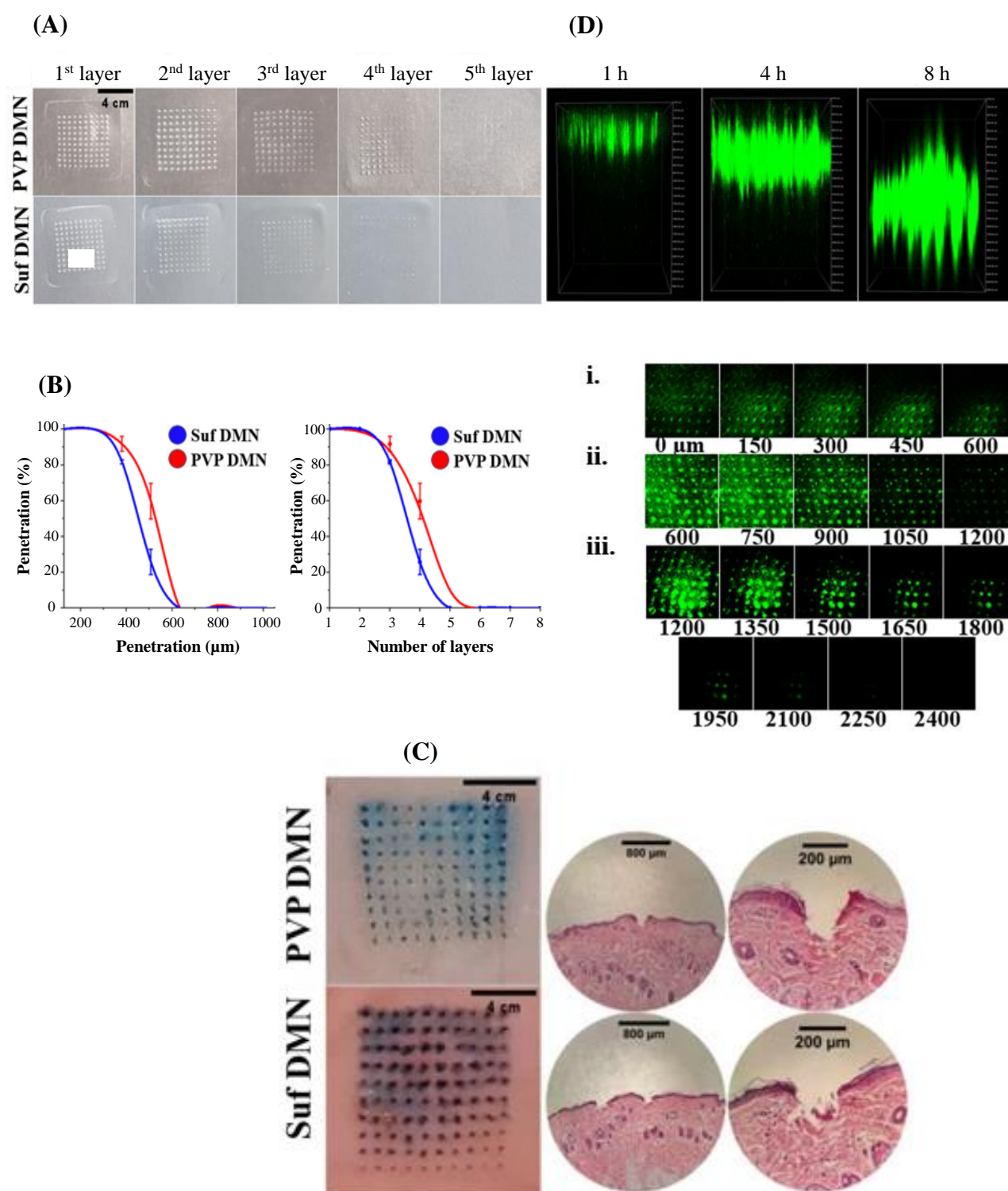
(A)

(B)

(C)

(D)

Fig. 2. Penetration test with DMNs. (A) Light microscopic images (1-5 layers) of DMN infiltration into PF layers. PVP DMNs penetrated the fourth layer of PF and SUF DMNs completely pierced the third layer (the thickness of each layer is 127 μm, with a dimension of 3 × 3 cm). (B) Percentage of each DMN penetration versus the number of PF layers and penetration depth. The total insertion depth is approximately 508 μm for PVP DMN and 381 μm for Suf DMN. The experiment was conducted in triplicates. (C) Insertion of trypan blue DMN and trypan blue/SUF DMN into mouse skin using H&E staining. (D) Transdermal administration of FITC DMN. Two-dimensional confocal microphotographs of FITC emission at different times after insertion (1, 4, and 8 h; for normalization of images, all images were taken at a depth of 2400 μm), the diffusion depth was (i) ~700 μm at 1 h, (ii) 1200 μm at 4 h, and (iii) ~2000 μm at 8 h after insertion.

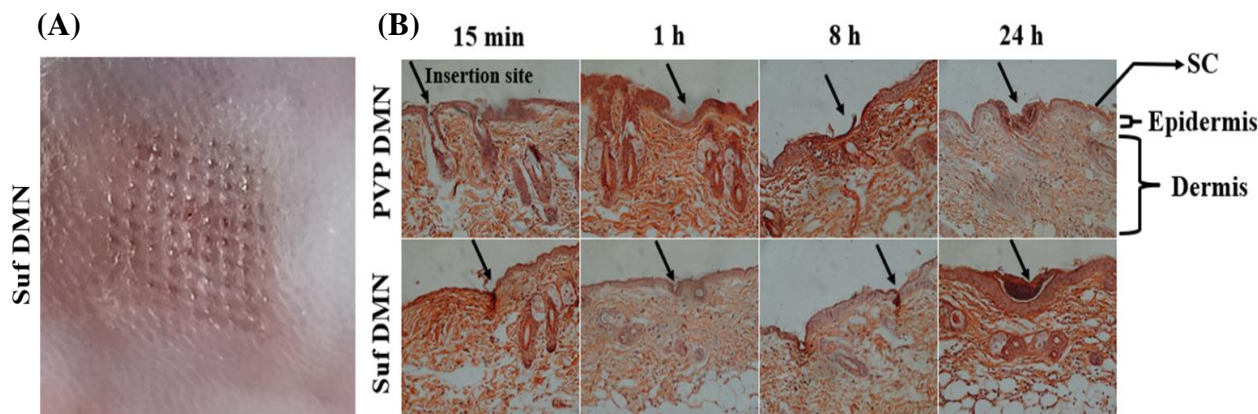**(A)**

(B)

Fig. 3. Inflammatory and histological examination of the skin. (A) Mild and transient skin irritation immediately after the removal of the DMN patch. (B) H&E images of the process of skin healing. As shown in the image, the depth of micropores decreases over time. Arrows indicate the perforated ducts and their closing process (Olympus BX61, Japan). SC: subcutaneous
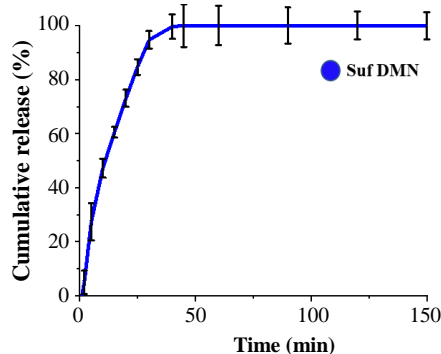

Fig. 4. Cumulative release percentage of SUF. Up to 60% of SUF is released within 15 min, which may be due to the suitable water solubility of PVP. About 84% is released within 25 min, and the cumulative percentage remains almost unchanged 45 min after initiation. The experiment was carried out in triplicates.

However, no significant difference was observed in dissolution between the microneedles with or without the drug ($p > 0.05$).

Anti-nociceptive effect of SUF

In examining the four animal groups using the hot plate technique, we observed no significant difference in anti-nociceptive activity between the SUF DMN group and the group that received SUF subcutaneously within 1 h of injection. In contrast, there was a significant difference between these two groups and the control groups ($p < 0.05$). However, over time, the effect of SUF DMN decreased. Also, at the end of the period, the SUF DMN group, but not the SUF subcutaneous group, lost its efficacy after 6 h (Fig. 8).

DISCUSSION

Herein, we fabricated SUF DMNs by a typical micro-molding process[26] with a height of 800 μm. In

agreement with our results, other studies have used pyramidal microneedles with the same height because of their proper mechanical strength[27].

The FTIR spectrum of the components of the constructed microneedle ranged between 500 and 4000 cm^{-1}, confirming the existence of functional groups of the DMN polymers and the interactions between the compounds of DMN. The FTIR results of our study aligns with those of another study[28].

Various tests indicated the proper physical resistance of PVP for skin infiltration[29], for this reason, we measured the mechanical strength of the PVP MN arrays using a compression test involving various predetermined forces generated by a tissue analyzer. Obtained data show the favorable mechanical strength of microneedles to withstand the maximum insertion force that a person would typically exert when puncturing the MN patches into the skin without an applicator. The application of artificial skin models solves challenges associated with biological skin test, including limited access to skin samples, the difficulty of stretching the skin into its in vivo configuration, and concerns about occupational safety and cost[30]. In an earlier investigation, PF has been used as a skin simulator and also as an alternative to biological tissues to analyze insertion depth[31]. Our results of in vivo PF insertion assay showed the proper potential of microneedle patch for SC penetration[32].

The DMNs are able to penetrate the subcutaneous of the skin sufficiently without breaking or bending during insertion[31]. In this context, several types of skin samples from rodents can be used for in vivo insertion analysis[31]. We inserted the DMN into rat skin to further verify the in vivo insertion of PVP MN. Application of a dye, such as trypan blue, to the skin surface or measurement of transepidermal water loss after the removal of MN can confirm whether the skin has been breached[31]. Trypan blue was used in our study to
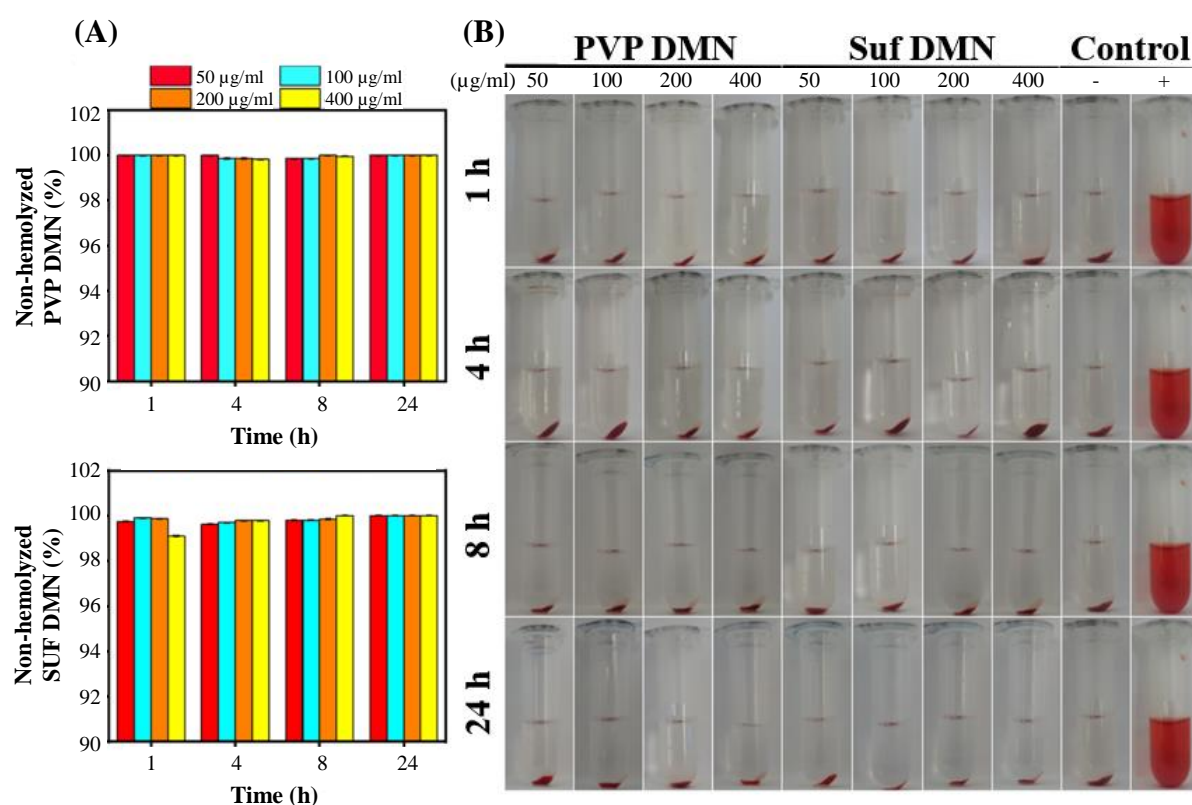
Fig. 5. Hemocompatibility test of DMNs. (A) Hemolysis percentage graph of the study groups vs. the negative control (PBS). As shown in all tested concentrations of both PVP DMNs and SUF DMNs, the results for non-hemolyzed erythrocytes were >99%, in contrast to the positive control with 100% erythrocyte lysis. (B) The transparency of supernatants in the tubes. Water was used as a positive control. The experiment was performed in four replicates.

measure the depth of permeation. The results of staining and confocal microscopy (FITC) both indicate the penetration of the microneedle into the hairless animal skin[33].

Since the microneedles are a minimally invasive tool, it is important to investigate local skin irritation and inflammatory reactions[34]. In this study, no erythema or inflammatory reactions were detected at the administration site, although mild and transient skin irritation was observed. The transient disruption of SC by the formation of micropores must be closed to prevent adverse physiological effects[35]; therefore, the timing of micropore closure is critical[36]. Our histological assessments of the skin for 24 h indicated that the depth of the micropores decreased over time. This data is in consistent with other studies performed on the closure of micropores resulting from microneedles application[37-41].

In our study, in vitro release assays revealed a time-dependent release profile for SUF. The initial release percentage of SUF was about 60% within 15 min. Du et al. also observed a time-dependent release profile for hyaluronic acid from their designed microneedle, with the accumulated release percentage of HA reaching up to 52% within 10 min. These findings are in agreement with our data and can be attributed to the appropriate water solubility of both compounds[42].

Hemocompatibility and the absence of erythrocyte lysis are two of the the most common biocompatibility assays[43]. Our data demonstrated an appropriate hemocompatibility for PVP and PVP/SUF polymers. This result is supported by the study that Elim and collogues performed on polymeric microneedle drug delivery systems[44]. We also examined the in vivo toxicity of SUF DMN and found no toxic effect in the serum or histological examination. The data from the toxicity tests in our study represented a consistency with the results of the study conducted by Chen et al. conducted on DPMN[40], exhibiting no significant erythrocyte lysis in DPMN samples[45].

Dissolution studies were also conducted to predict the time needed for drug release from DMN arrays. The DMNs fabricated using PVP as the primary polymer dissolve quickly in the skin[46]. In our study, when a supporter was used, almost 50% of the arrays dissolved
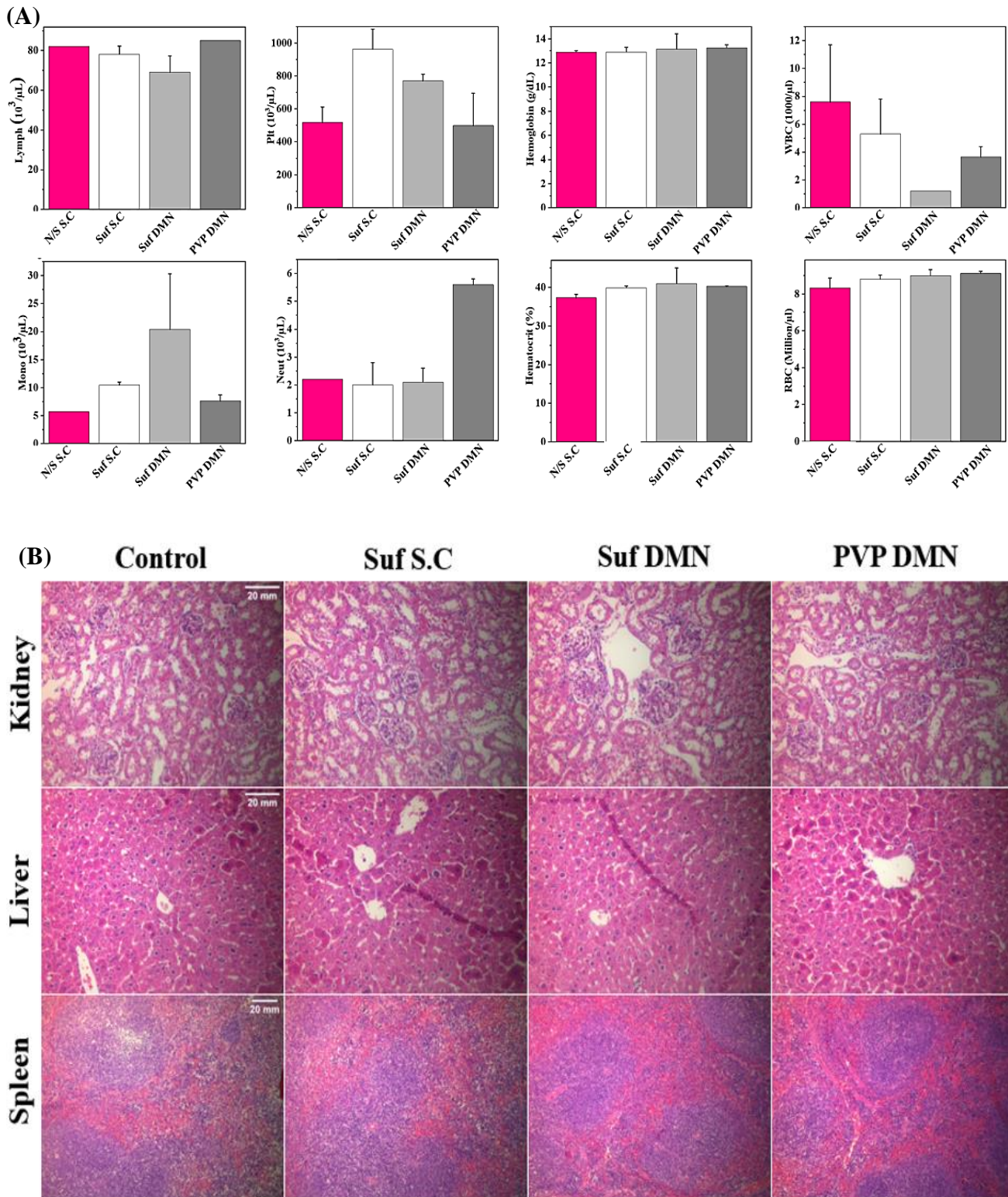
(A)

(B)

Fig. 6. In vivo toxicity assay. (A) Graph of hematological parameter assay in the studied groups. No statistical difference was observed between the control group (N/S SC) and the treated groups (SUF SC, SUF DMN, and PVP DMN) for each of the parameters (data reported as mean ± SD; one-way ANOVA, Tukey post hoc ($p > 0.05$). The experiment was performed in triplicates. (B) H&E staining of the kidney, liver, and spleen of mice 14 days after treatment. No noticeable histopathological abnormalities or damage were detected in the experimental groups compared to the control group. SC: subcutaneous
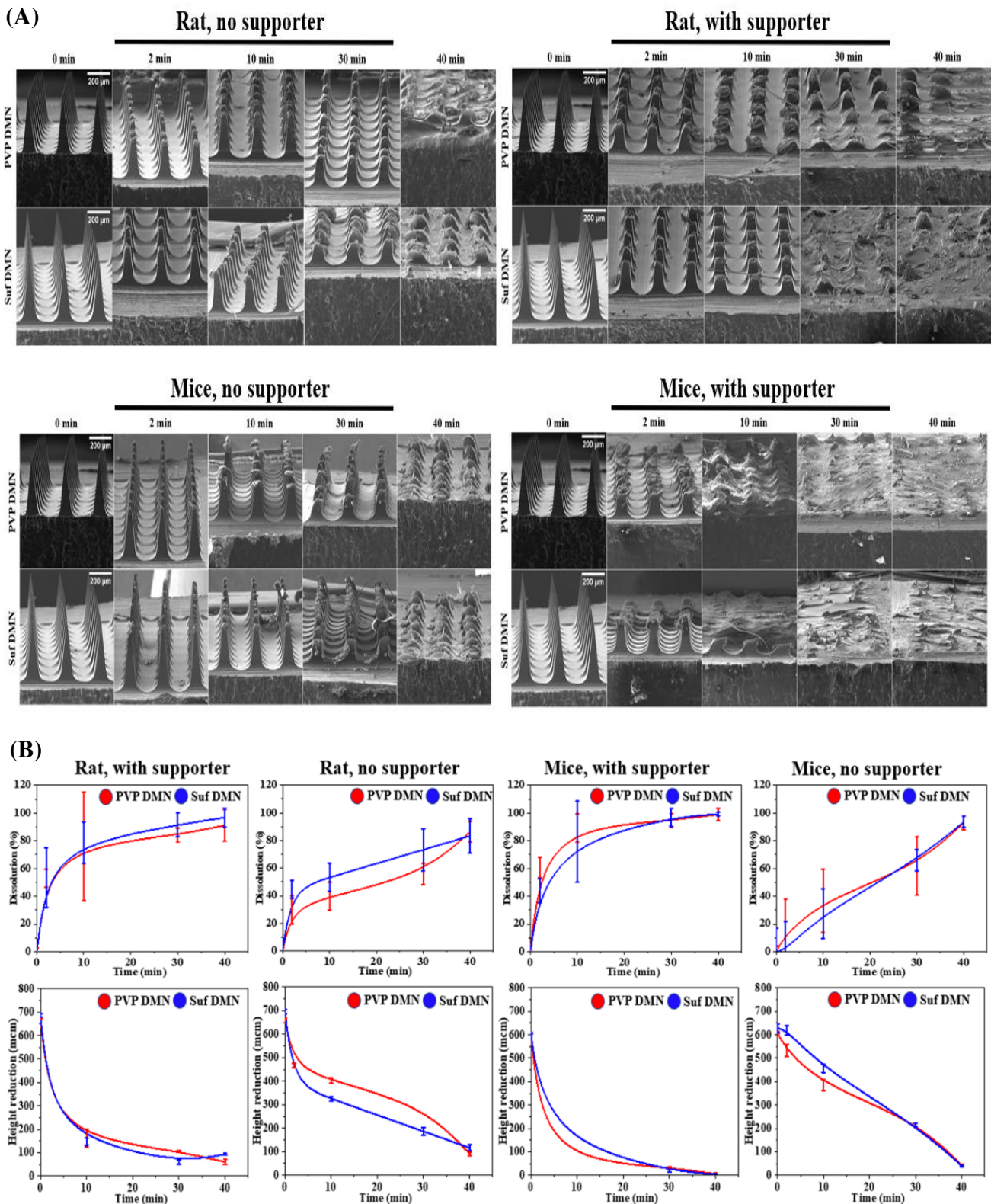
Fig. 7. In vivo transdermal dissolution test. The (A) image and (B) graph of microneedle dissolution in different experimental groups. The DMNs exhibit different results in the presence or absence of supporter. The difference in the thickness of the animal's skin also significantly affected the dissolution ($p < 0.05$); the experiment was performed in triplicates. On the other hand, in each group, there was no significant difference between the microneedles containing the drug and those without the drug ($p > 0.05$).

in the skin of both animals within 5 min after insertion, while they were entirely dissolved within 20 min. Dissolution time in our study is longer than other PVP MNs, showing a sustained drug release. This discrepancy could be due to the differences in the manufacturing method[47]. The hot plate technique is one of the common methods used for pain assessment. The subcutaneous administration is a conventional method for prescribing SUF, a potent opioid with a rapid analgesic effect[48]. Data obtained from hot plate test showed a significant difference between the control group and the group administrated with SUF. However, no significant difference in response to the hot plate was observed between the SUF DMN group and the subcutaneous SUF group. In general, our proposed microneedle provides adequate analgesic effects.
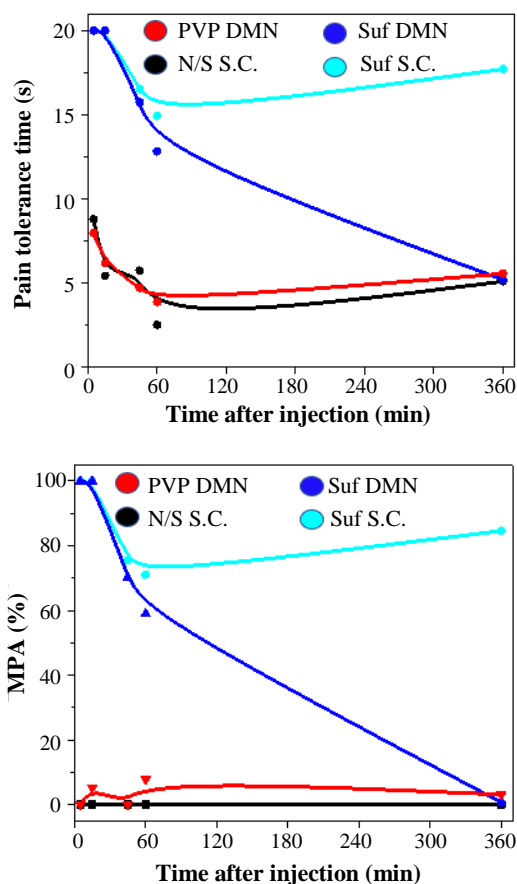

Fig. 8. The graph of hot plate test. Jumping times of mice on the surface of the hot plate (55 °C ± 0.1) were recorded. Test was performed on four different groups of male mice (n = 6 in each group, weighing 18-22 g). The cut-off time was 20 s. The percentage of MPA was calculated for each group. There was no significant difference in hot plate response between the SUF DMN group and the group received subcutaneous SUF within 1 h of injection. However, a significant difference was observed between these two groups and the control groups ($p < 0.05$). From 6 h, the SUF DMN group also lost its efficacy in pain control, with a notable difference from the subcutaneous SUF group ($p < 0.05$).

CONCLUSION

In this study, we successfully developed a rapid dissolving PVP microneedle using micromolding technique for transdermal delivery of SUF. The in vitro and in vivo evaluation of the DMNs exhibited satisfying characteristics in terms of mechanical properties, skin penetration, chemical structure, drug release, and microneedle formulation, with respect to blood compatibility and histological assessments. Our study highlights the effectiveness of microneedle-mediated pain management for providing immediate pain relief as a substitute for traditional pain control methods, without complications associated with opioids.

DECLARATIONS

Acknowledgments

Ethical approval
All the experimental procedures in this study were conducted in accordance with the Institutional Animal Care guidelines of ARRIVE guidelines in animal experiments and according to the U.K. Animals (Scientific Procedures) Act, 1986, and associated guidelines, EU Directive 2010/63/EU for animal experiments. The American Veterinary Medical Association (AVMA) easy euthanasia technique was used in the present research. The study protocol was approved by the Research Ethics Committee of Zanjan University of Medical Sciences, Zanjan, Iran (ethical code: IR. ZUMS. REC.1399.203).

Consent to participate
Not applicable.

Consent for publication
All authors reviewed the results and approved the final version of the manuscript.

Authors' contributions
ZP: performed the laboratory assessments, performed in vivo assessments and data analysis, and wrote the manuscript; AM, MT, and MA: performed the laboratory assessments; MAS: performed the conception of the article and reviewed and edited the article; AR: performed in vivo assessments and data analysis, reviewed and edited the article.

Data availability

All relevant data can be found within the manuscript.

Competing interests

The authors declare that they have no competing interests.

Supplementary information

The online version contains supplementary material.

REFERENCES

1. Merskey HJP. Pain terms: a list with definitions and notes on usage. Recommended by the IASP Subcommittee on Taxonomy. Pain. 1979; 6:249-52.
2. Kerrigan S, Goldberger BA. Opioids. Principles of forensic toxicology. first ed: Springer; 2020. p. 347-69.
3. Maurya A, Rangappa S, Bae J, Dhawan T, Ajjarapu SS, Murthy SN. Evaluation of soluble fentanyl microneedles for loco-regional anti-nociceptive activity. Int J Pharm. 2019; 564:485-91.
4. Porela-Tiihonen S, Kokki H, Kokki MJEOoP. An up-to-date overview of sublingual sufentanil for the treatment of moderate to severe pain. Expert Opin Pharmacother. 2020; 21(12):1407-18.
5. Wang Y, Xu W, Xia W, Wei L, Yang D, Deng X, et al. Comparison of the Sedative and Analgesic Effects of dexmedetomidine–remifentanil and dexmedetomidine–dufentanil for liposuction: A prospective single-blind Randomized Controlled Study. Aesthetic Plast Surg. 2022; 46(1):524-34.
6. Sridharan K, Sivaramakrishnan GJCcp. Comparison of fentanyl, remifentanil, sufentanil and alfentanil in combination with propofol for general anesthesia: a systematic review and meta-analysis of randomized controlled trials. Curr Clin Pharmacol. 2019; 14(2):116-24.
7. Fang P, Qian J, Ding J, Pan X, Su H, Liu XJP, et al. Comparison of analgesic effects between nalbuphine and sufentanil in first-trimester surgical abortion: a randomized, double-blind, controlled trial. Pain Ther. 2022; 11(1):121-32.
8. Van de Donk T, Ward S, Langford R, Dahan AJA. Pharmacokinetics and pharmacodynamics of sublingual sufentanil for postoperative pain management. Anaesthesia. 2018; 73(2):231-7.
9. Zhao L, Li YJOL. Application of dexmedetomidine combined with sufentanil in colon cancer resection and its effect on immune and coagulation function of patients. Oncol Lett. 2020; 20(2):1288-94.
10. Bovill JG, Sebel PS, Blackburn CL, Oei-Lim V, Heykants JJJA. The pharmacokinetics of sufentanil in surgical patients. Anesthesiology 1984; 61(5):502-6.
11. Ahonen J, Olkkola KT, Hynynen M, Seppälä T, Ikävalko H, Remmerie B, et al. Comparison of alfentanil, fentanyl and sufentanil for total intravenous anaesthesia with propofol in patients undergoing coronary artery bypass surgery. Br J Anaesth. 2000; 85(4):533-40.
12. Pichini S, Solimini R, Berretta P, Pacifici R, Busardò FPJTdm. Acute intoxications and fatalities from illicit fentanyl and analogues: an update. Ther Drug Monit. 2018; 40(1):38-51.
13. Fisher DM, Chang P, Wada DR, Dahan A, Palmer PPJA. Pharmacokinetic properties of a sufentanil sublingual tablet intended to treat acute pain. Anesthesiology. 2018; 128(5):943-52.
14. Bui VD, Son S, Xavier W, Jung JM, Lee J, Shin S, et al. Dissolving microneedles for long-term storage and transdermal delivery of extracellular vesicles. Biomaterials. 2022; 287:121644.
15. Oosten AW, Abrantes JA, Jönsson S, de Bruijn P, Kuip EJ, Falcão A, et al. Treatment with subcutaneous and transdermal fentanyl: results from a population pharmacokinetic study in cancer patients. Eur J Clin Pharmacol. 2016; 72:459-67.
16. Wang Q, Yang X, Gu X, Wei F, Cao W, Zheng L, et al. Celecoxib nanocrystal-loaded dissolving microneedles with highly efficient for osteoarthritis treatment. Int J Pharm. 2022; 625:122108.
17. Makvandi P, Jamaledin R, Chen G, Baghbantaraghdari Z, Zare EN, Di Natale C, et al. Stimuli-responsive transdermal microneedle patches. Materials Today. 2021; 47:206-22.
18. Ray S, Wirth DM, Ortega-Rivera OA, Steinmetz NF, Pokorski JKJB. Dissolving microneedle delivery of a prophylactic HPV vaccine. Biomacromol 23. 2022; 23(3):903-12.
19. Paredes AJ, Volpe-Zanutto F, Vora LK, Tekko IA, Permana AD, Picco CJ, et al. Systemic delivery of tenofovir alafenamide using dissolving and implantable microneedle patches. Materials Today Bio. 2022; 13:100217.
20. Prausnitz MR, Mitragotri S, Langer RJNrDd. Current status and future potential of transdermal drug delivery. Nat Rev Drug Discov. 2004; 3(2):115-24.
21. Damiri F, Kommineni N, Ebhodaghe SO, Bulusu R, Jyothi VGS, Sayed AA, et al. Microneedle-based natural polysaccharide for drug delivery systems (DDS): progress and challenges. Pharmaceuticals. 2022; 15(2):190.
22. Kim MJ, Seong K-Y, Jeong JS, Kim SY, Lee S, Yang SY, et al. Minoxidil-loaded hyaluronic acid dissolving microneedles to alleviate hair loss in an alopecia animal model. Acta Biomater. 2022; 143:189-202.
23. Abdelghany S, Alshaer W, Al Thaher Y, Al Fawares M, Al-Bakri AG, Zuriekat S, et al. Ciprofloxacin-loaded dissolving polymeric microneedles as a potential therapeutic for the treatment of S. aureus skin infections. Beilstein J Nanotechnol. 2022; 13(1):517-27.
24. Anjani QK, Sabri AHB, Utomo E, Domínguez-Robles J,

Donnelly RFJMP. Elucidating the impact of surfactants on the performance of dissolving microneedle array patches. Mol Pharmaceutics. 2022; 19(4):1191-208.

25. Eddy NB, Leimbach D. Synthetic analgesics. II. Dithienylbutenyl-and dithienylbutylamines. J Pharmacol Exp Ther. 1953; 107(3):385-93.

26. Malek-Khatabi A, Rad ZF, Rad-Malekshahi M, Akbarijavar H. Development of dissolvable microneedle patches by CNC machining and micromolding for drug delivery. Mater Lett. 2023; 330:133328.

27. Koh KJ, Liu Y, Lim SH, Loh XJ, Kang L, Lim CY, et al. Formulation, characterization and evaluation of mRNA-loaded dissolvable polymeric microneedles (RNApatch). Sci Rep. 2018; 8(1):11842.

28. Safo I, Werheid M, Dosche C, Oezaslan MJNA. The role of polyvinylpyrrolidone (PVP) as a capping and structure-directing agent in the formation of Pt nanocubes. Nanoscale Adv 2019; 1(8):3095-106.

29. Tran L-G, Park W-T. Rapid biodegradable microneedles with allergen reservoir for skin allergy test. Micro and Nano Syst Lett. 2020; 8(11):1-5.

30. Flaten GE, Palac Z, Engesland A, Filipović-Grčić J, Vanić Ž, Škalko-Basnet NJEjops. In vitro skin models as a tool in optimization of drug formulation. 2015; 75:10-24.

31. Makvandi P, Kirkby M, Hutton AR, Shabani M, Yiu CK, Baghbantaraghdari Z, et al. Engineering microneedle patches for improved penetration: analysis, skin models and factors affecting needle insertion. Nanomicro Lett. 2021; 13(1):1-41.

32. Czekalla C, Schönborn KH, Lademann J, Meinke MC. Noninvasive determination of epidermal and stratum corneum thickness in vivo using two-photon microscopy and optical coherence tomography: impact of body area, age, and gender. Skin Pharmacol Physiol. 2019; 32(3):142-50.

33. Kathuria H, Kang K, Cai J, Kang LJIJoP. Rapid microneedle fabrication by heating and photolithography. Int J Pharm. 2020; 575:118992.

34. Chen M-C, Lin Z-W, Ling M-HJAn. Near-infrared light-activatable microneedle system for treating superficial tumors by combination of chemotherapy and photothermal therapy. ACS nano. 2016; 10(1):93-101.

35. Kelchen MN, Siefers KJ, Converse CC, Farley MJ, Holdren GO, Brogden NKJJocr. Micropore closure kinetics are delayed following microneedle insertion in elderly subjects. Journal of controlled release. 2016; 225:294-300.

36. Gupta J, Gill HS, Andrews SN, Prausnitz MRJJocr. Kinetics of skin resealing after insertion of microneedles in human subjects. Journal of controlled release. 2011; 154(2):148-55.

37. Nagra U, Barkat K, Ashraf MU, Shabbir MJD-R.

Feasibility of enhancing skin permeability of acyclovir through sterile topical lyophilized wafer on self-dissolving microneedle-treated skin. Dose Response. 2022; 20(2):15593258221097594.

38. Chen MC, Lai KY, Ling MH, Lin C-WJAb. Enhancing immunogenicity of antigens through sustained intradermal delivery using chitosan microneedles with a patch-dissolvable design. Acta biomaterialia. 2018; 65:66-75.

39. Zhao X, Li X, Zhang P, Du J, Wang YJJocr. Tip-loaded fast-dissolving microneedle patches for photodynamic therapy of subcutaneous tumor. J Controlled Release. 2018; 286:201-9.

40. Chen MC, Huang SF, Lai KY, Ling MHJB. Fully embeddable chitosan microneedles as a sustained release depot for intradermal vaccination. Biomaterials. 2013; 34(12):3077-86.

41. Chen YH, Lai KY, Chiu YH, Wu YW, Shiau AL, Chen MCJAB. Implantable microneedles with an immune-boosting function for effective intradermal influenza vaccination. Acta biomaterialia. 2019; 97:230-8.

42. Du H, Liu P, Zhu J, Lan J, Li Y, Zhang L, et al. Hyaluronic acid-based dissolving microneedle patch loaded with methotrexate for improved treatment of psoriasis. ACS Appl Mater Interfaces. 2019; 11(46):43588-98.

43. Xing M, Liu H, Meng F, Ma Y, Zhang S, Gao YJP. Design and evaluation of complex polypeptide-loaded dissolving microneedles for improving facial wrinkles in different areas. Polymers. 2022; 14(21):4475.

44. Elim D, Fitri AMN, Mahfud MASb, Afika N, Sultan NAF, Asri RM, et al. Hydrogel forming microneedle-mediated transdermal delivery of sildenafil citrate from polyethylene glycol reservoir: An ex vivo proof of concept study. Colloids Surf B Biointerfaces. 2023; 222:113018.

45. Chen Y, Yang Y, Xian Y, Singh P, Feng J, Cui S, et al. Multifunctional graphene-oxide-reinforced dissolvable polymeric microneedles for transdermal drug delivery. ACS Appl Mater Interfaces. 2019; 12(1):352-60.

46. Ramöller IK, Tekko IA, McCarthy HO, Donnelly RFJIJoP. Rapidly dissolving bilayer microneedle arrays–a minimally invasive transdermal drug delivery system for vitamin B12. Int J Pharm. 2019; 566:299-306.

47. Duan X, Ma J, Ning M, Gao Y. Dissolving Microneedles Loaded with Gestodene: Fabrication and characterization In vitro and in vivo. Iran J Pharm Res. 2023; 22(1):e131819.

48. Fisher DM, Kellett N, Lenhardt RJTJotASoA. Pharmacokinetics of an implanted osmotic pump delivering sufentanil for the treatment of chronic pain. Anesthesiology. 2003; 99(4):929-37.